

This is the accepted manuscript made available via CHORUS. The article has been published as:

# Density functional methods for the magnetism of transition metals: SCAN in relation to other functionals

Yuhao Fu and David J. Singh

Phys. Rev. B **100**, 045126 — Published 18 July 2019

DOI: [10.1103/PhysRevB.100.045126](https://doi.org/10.1103/PhysRevB.100.045126)

# Density Functional Methods for the Magnetism of Transition Metals: SCAN in Relation to Other Functionals

Yuhao Fu<sup>1</sup> and David J. Singh<sup>1,\*</sup>

<sup>1</sup>*Department of Physics and Astronomy, University of Missouri, Columbia, MO 65211-7010 USA*

(Dated: June 24, 2019)

We report tests of various density functionals for ferromagnetic, Fe, Co and Ni with a focus on characterizing the behavior of the so-called strongly constrained and appropriately normed (SCAN) functional. It is found that SCAN is closer in behavior to functionals that yield localized behavior, such as hybrid functionals, than other semilocal functionals that are tested. The results are understood in terms of a tendency to differentiate orbitals, favoring integer occupation, which is necessary for a correct description of atomic systems, but inappropriate for the open shell metallic ferromagnetic metals studied here. Not only is the exchange splitting for open shells enhanced with SCAN, but as seen in Ni, there is much more band dependence, with significantly more overestimation for bands corresponding to the partially filled orbitals.

## I. INTRODUCTION

The 3d transition metals and their compounds present an exceptional range of physical behavior in part because of the possibility for the 3d electrons to be localized, itinerant or in between. Examples of this rich physics include the band structure related magnetism of elemental Fe, Co and Ni, the Mott insulating physics of many transition metal oxides, and the apparently distinct high temperature superconductivity of cuprates and Fe-pnictides. A long standing goal has been the development of predictive theories, and in particular, computationally tractable theories that can reliably capture the physics of this range of materials. The challenge to theory is to develop density functionals that can describe both localized and itinerant behavior in a predictive way. In this regard, the concept of “Jacob’s Ladder” has become widely held. In this view, adding more ingredients in density functionals, and constraining this added flexibility by appropriate exact relations should give overall more accurate descriptions of atoms, molecules and solids.<sup>1–3</sup>

It has long been recognized that functionals such as the local (spin) density approximation (LDA) and standard generalized gradient approximations (GGAs) do not provide an adequate treatment of correlated 3d oxides such as the Mott insulating parents of the cuprate superconductors.<sup>4,5</sup> This is due to an inadequate treatment of correlations, which can be traced to self-interaction errors,<sup>6</sup> and an insufficient tendency towards integer orbital occupations. This is the basis for methods that add a Hubbard  $U$  correction, i.e. LDA+ $U$ .<sup>7,8</sup> It is also a key aspect of a correct description of atoms and molecules, where it can be traced to the need for a correct description of the exchange correlation energy as a function of occupation number in order to avoid delocalization errors.<sup>9–11</sup> These delocalization errors can also be reduced by hybrid functionals, which can also correctly predict an antiferromagnetic insulating ground state for Mott insulators, including the high- $T_c$  parent,  $\text{La}_2\text{CuO}_4$ .<sup>11–14</sup> These incorporate explicit orbital dependence, and have been very important in the description

of semiconductors, where in addition to improved ground state properties they also improve band gaps.

Recently, a semi-local meta-GGA functional, including the local (spin) densities, gradients and a kinetic energy density was proposed. This is the so-called strongly constrained and appropriately normed (SCAN) functional.<sup>15,16</sup> Advantages of this meta-GGA approach include the fact that calculations using a meta-GGA are computationally much less demanding than hybrid functional calculations for solids, the kinetic energy density can provide information about orbital character, and calculations of energetics for diverse systems showed that the SCAN functional provides improvements over other functionals for a wide variety of solid state and molecular properties.<sup>16–19</sup> Significantly, based on calculations, unlike GGAs, this functional is able to describe the ground state of  $\text{La}_2\text{CuO}_4$  at least qualitatively.<sup>20</sup>

Thus is reasonable to suppose that the SCAN functional provides an overall improvement in the description of transition metals and compounds. However, recent results, especially for Fe, Co and Ni, show this not to be the case.<sup>19,21–23</sup> In particular, the magnetic tendency of these ferromagnetic metals is strongly overestimated, as are the magnetic energies. This is particularly severe in the case of Fe. In that case the large errors make the SCAN functional incapable of describing the phase stabilities underlying the materials science of steel.<sup>23</sup>

Here we compare SCAN with other functionals for these transition metal ferromagnets. The results show the origin of the problems in the SCAN treatment of these materials is in the differentiation of orbitals. This is particularly seen in Ni where the exchange splitting is strongly enhanced in particular for bands corresponding to partially filled orbitals, leading to large errors for the band crossing the Fermi level at the  $X$ -point, while enhancing the exchange splitting of occupied bands much more weakly. This is in contrast to standard semilocal functionals that give much more similar exchange splittings for the different bands. This underscores the difficulty of finding a functional that can treat the full range of transition metal magnets. Such a functional must in-

clude the atomic physics favoring integer occupations in Mott insulators, such as undoped cuprates, and also the tendency towards multi-orbital open shell behavior materials that have significant itinerancy, such as Fe and Fe-based superconductors.<sup>24</sup> Thus the problem of developing a functional that properly describes both localized electron behavior and itinerant behavior remains to be solved.

## II. COMPUTATIONAL METHODS

We performed first principles calculations with several different exchange-correlation functionals. These were the LDA, the PBE GGA,<sup>25</sup> the SCAN,<sup>15</sup> TPSS<sup>26</sup> and revTPSS meta-GGAs,<sup>27,28</sup> and the HSE03,<sup>29,30</sup> HSE06<sup>31</sup> and PBE0<sup>32,33</sup> hybrid functionals. We additionally performed PBE+ $U$  calculations with various choices of the Hubbard parameter,  $U$ .

We used two different methods, specifically the projector augmented wave (PAW) method as implemented in the VASP code,<sup>34,35</sup> and the all electron general potential linearized augmented plane wave (LAPW) method,<sup>36</sup> as implemented in the WIEN2K code.<sup>37</sup> Here we focus on results at the experimental lattice parameters in order to better compare the description of magnetism in different approaches. These are  $a=2.860$  Å, for bcc Fe,  $a=3.523$  Å, for fcc Ni and  $a=2.507$  Å,  $c=4.070$  Å, for hcp Co. The dependencies on lattice parameter for Fe comparing SCAN, PBE and LDA were presented previously.<sup>23</sup>

The VASP and WIEN2k codes have different implementations of the meta-GGA functionals, which involve different approximations. VASP implements self-consistent calculations, but requires the use of PAW pseudopotentials, which are not available for the meta-GGA functionals. As such, we relied on PBE GGA PAW pseudopotentials, which is an approximation. The general potential LAPW method, implemented in WIEN2k, is an all-electron method, and does not use pseudopotentials. Additionally, WIEN2k has an efficient implementation of the fixed spin moment constrained density functional theory method.<sup>38,39</sup> This allows calculation of the magnetic energy as a function of the imposed magnetization, which provides additional information about the behavior of the functionals, and also facilitates determination of the magnetic contribution to the energy. However, WIEN2k does not provide a self-consistent calculation with meta-GGA potentials, and instead the energy is calculated for densities obtained with the PBE GGA. This is an approximation for the energies, and also prevents calculation of the electronic band structures with the meta-GGA potentials. We find that the approximations above are not significant for the energies of the transition metals discussed here. A comparison of the different methods for Fe is presented in Table I.

In addition, as a test we did calculations for Fe using the ELK code.<sup>40</sup> This code has a self-consistent implementation of the SCAN functional. We obtain a

TABLE I. Comparison of results for bcc Fe at the experimental lattice parameters using VASP and WIEN2k as employed here (see text).

		LDA	PBE	SCAN
VASP	$m_{sp}$ ( $\mu_B$ )	2.15	2.25	2.65
	$\Delta E_{mag}$ (meV)	-411	-571	-1081
WIEN2k	$m_{sp}$ ( $\mu_B$ )	2.20	2.21	2.63
	$\Delta E_{mag}$ (meV)	-442	-561	-1114

spin magnetic for Fe of  $2.64 \mu_B$  with SCAN using this code. This is in excellent agreement with the VASP and WIEN2k results, supporting the accuracy of the present calculations.

The PAW calculations were done with a planewave kinetic energy cut-off of 400 eV. We used converged, tested Brillouin zone samplings, based on uniform meshes. The LAPW calculations were done with sphere radii of  $R=2.25$  Bohr and basis sets defined by  $RK_{max}=9$ , where  $K_{max}$  is the planewave sector cut-off. Local orbitals were used to treat semicore states. These are standard settings.

For the PBE+ $U$  calculations, we used different values of  $U$ , with the standard procedure of Dudarev and co-workers,<sup>41</sup> and the fully localized limit (SIC) double counting. We covered the range up to  $U=8$  eV. It is common to find values in range of  $U=5$  eV to  $U=8$  eV employed, in literature for  $3d$  transition metal compounds. This is based in part on the view that  $U$  is a local atomic quantity that describes correlation effects that are missing in calculations with standard density functionals, such as the LDA or PBE GGA, and therefore does not have much system dependence.

This view has been criticized, however, and procedures have been developed for determining  $U$  for particular systems. These are based on constrained calculations changing the electron occupation of the orbital of interest, or by linear response.<sup>42,43</sup> This is important because screening, which strongly reduces  $U$  from its bare atomic value, varies from system to system. For our purpose, it is important to note that these methods for obtaining  $U$  are designed to improve the description of the energy variation between integer orbital occupations, i.e. line segments connecting the values at integer occupations.

In any case, we also estimated values of  $U$  using the linear response method implemented in Quantum ESPRESSO. These estimated values are 4.33 eV for Fe, 2.62 eV for Co and 5.56 eV for Ni. While the basis set and implementation of PBE+ $U$  in the LAPW method and the pseudopotential planewave method of Quantum ESPRESSO are different, so that values cannot be directly translated, these do provide an indication of the rough values and we present also calculations for these specific values. Importantly, these values are never zero, although, as discussed below, a value of zero gives the best agreement with experiment for these elemental transition metal ferromagnets.

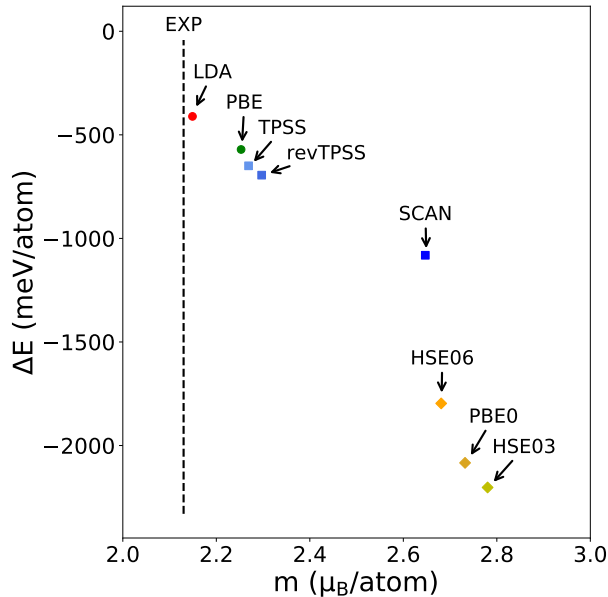


FIG. 1. The calculated magnetic energy and spin magnetizations of bcc Fe. The magnetic energy is defined as the difference in energy between the non-spin-polarized and ferromagnetic ground state. The calculations were done self-consistently, using VASP for the LDA, GGA and meta-GGA functionals and WIEN2k for the hybrid functionals.

### III. RESULTS AND DISCUSSION

We begin with bcc Fe. Figure 1 shows our results for the magnetic energy of bcc Fe with different exchange-correlation functionals, at its experimental lattice parameter. Numerical values and magnetic moments are given in Table II.

The experimental spin magnetizations of Fe, Co and Ni are  $2.13 \mu_B$ ,  $1.57 \mu_B$  and  $0.57 \mu_B$  per atom, respectively. As noted previously, the LDA and PBE GGA functionals provide values in good accord with experiment, while the SCAN meta-GGA was found to provide values significantly higher than experimental values.<sup>21,23</sup> This is why SCAN is unable to describe the phase balance that is central to the materials science of steel.<sup>23</sup> Furthermore, although the overestimates of the magnetization with SCAN amount to  $\sim 25\%$  for Fe, the magnetic energies were found to be greatly enhanced, by factors of two or more in these metals. Moreover, as seen in Fig. 1, the SCAN meta-GGA behaves quite differently than the other meta-GGA functionals, TPSS and revTPSS. Those functionals also enhance the magnetic tendency of Fe relative to the PBE GGA, but to a much smaller extent than SCAN. This is consistent with the previously noted improved description of correlated materials using SCAN, and underscores the difficulty of correctly describing both types of behavior with a single method.

It is also important to note that the already overestimated magnetic moments and energies with SCAN are

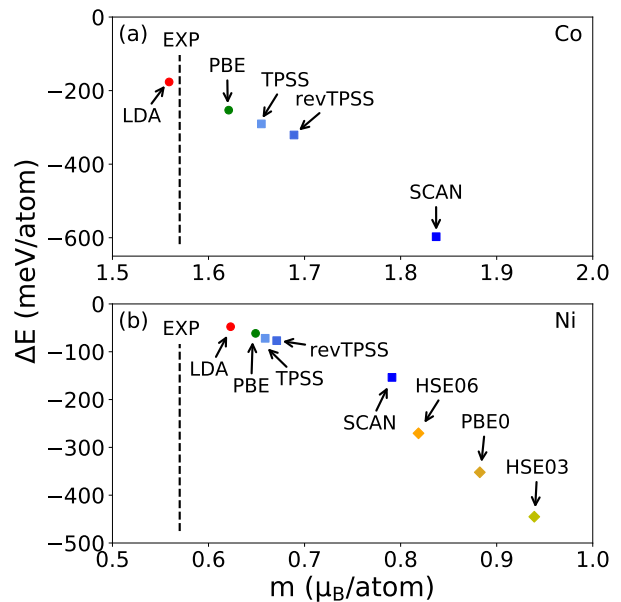


FIG. 2. Magnetic energy and spin magnetization per atom of hcp Co (top) and fcc Ni (bottom) as obtained with different functionals. The LDA, PBE GGA and meta-GGA calculations were done with VASP, and the hybrid functional calculations were done with WIEN2k.

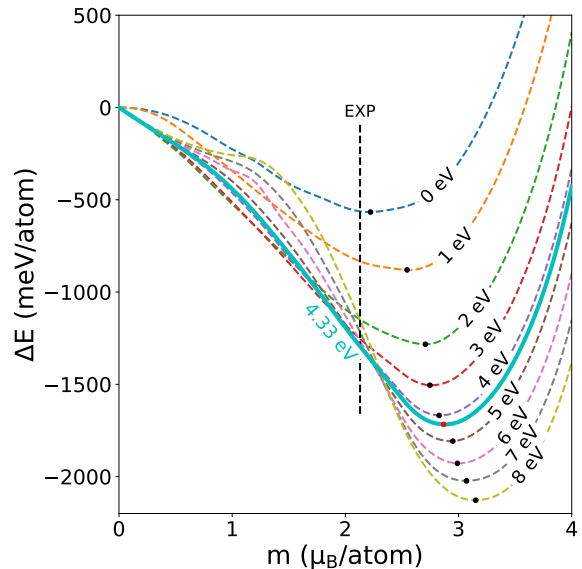


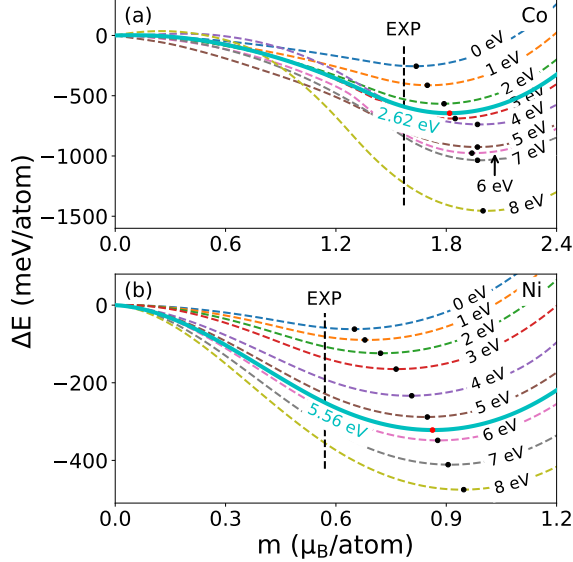
FIG. 3. Fixed spin moment energy as a function of spin magnetization per atom for bcc Fe, as obtained with the PBE+ $U$  method implemented in WIEN2k.

further enhanced with hybrid functionals, which also describe the localized electron behavior of correlated oxides, including FeO.<sup>14,44–46</sup> This enhancement is both in terms of moments, as was previously noted,<sup>47–49</sup> and also even more strongly in terms of magnetic energies.

We find similar results for Co and Ni. Spin magneti-

TABLE II. Properties of bcc Fe at its experimental lattice parameter ( $a_{exp}$ ) and its calculated lattice parameter ( $a_{cal}$ ).

	LDA	PBE	TPSS	revTPSS	SCAN	HSE06	PBE0	HSE03	Expt.
$a_{cal}$ (Å)	2.75	2.83	2.80	2.80	2.84	...	...	...	2.86
$m_{sp}$ ( $a_{exp}$ ) ( $\mu_B$ )	2.15	2.25	2.27	2.30	2.65	2.68	2.73	2.78	2.13
$m_{sp}$ ( $a_{cal}$ ) ( $\mu_B$ )	1.93	2.20	2.15	2.16	2.57	...	...	...	...
$\Delta E_{mag}$ ( $a_{exp}$ ) (meV)	-411	-571	-650	-695	-1081	-1797	-2202	-2084	...
$\Delta E_{mag}$ ( $a_{cal}$ ) (meV)	-279	-528	-567	-598	-1028	...	...	...	...

FIG. 4. Fixed spin moment energy as a function of spin magnetization per atom for Co and Ni, as obtained with the PBE+ $U$  method implemented in WIEN2k.

zations and magnetic energies are shown in Fig. 2. The main difference is that there is a greater relative overestimation of the moments with the TPSS and revTPSS meta-GGA functionals as compared to the PBE GGA.

As mentioned, another highly effective approach for localized systems is the addition of a Hubbard  $U$  correction, as in the widely used LDA+ $U$  and PBE+ $U$  schemes. The correction is designed to better distinguish orbitals, favoring integer occupation, and thus correct delocalization errors in standard LDA and GGA calculations. In this sense these Hubbard corrections have physics related to that of hybrid functionals, though with lower cost. As shown in Figs. 3 and 4, they do not improve results for magnetism in Fe, Co and Ni. This had been noted previously for the moment of Fe by Cococcioni and de Gironcoli who found an overestimation by  $\sim 20\%$  in LDA+ $U$  calculations.<sup>43</sup> We find here that this overestimation is general and also very strongly affects the magnetic energy.

It is important to note that PBE+ $U$  strongly degrades agreement with experiment for the values of  $U$  obtained from linear response and even for small values of  $U$ , e.g. 1 eV or 2 eV. Thus the addition of a static Hubbard correction degrades agreement with experiment for these

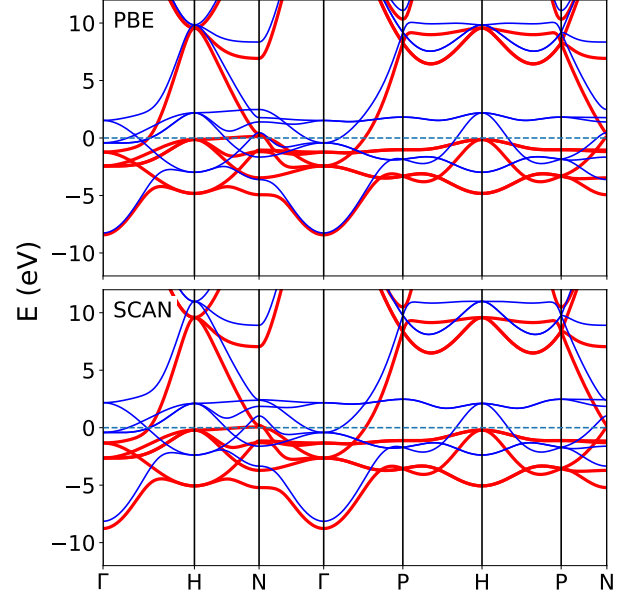


FIG. 5. Band structure of bcc Fe comparing PBE and SCAN, as obtained from self-consistent calculations with VASP. The Fermi level is at 0 eV and majority (minority) spin are shown as heavy red (light blue).

metals even if the correction is made small.

The Kohn-Sham eigenvalues in DFT do not correspond directly with experimental excitation energies, and therefore care should be taken in their interpretation. Nonetheless, within Kohn-Sham theory, they do control the occupancy of the Kohn-Sham orbitals and therefore the ground state properties, such as energy and magnetization. For example, enhancing exchange splitting while keeping the band width fixed will increase the magnetization. As such, analysis of the band structures can provide useful insights into the behavior of a functional.

It was observed that the  $d$  states of Fe are shifted to lower energy compared to the PBE GGA, due to an increased exchange splitting, which disagrees with experiment.<sup>19,21</sup> This is closely connected with the larger magnetization, since if the bands are relatively undistorted, the exchange splitting and magnetization will be closely related. Figs. 5 and 6 show our band structures with PBE and SCAN for Fe and Ni. As noted by Ekholm and co-workers, the the band widths using SCAN and PBE are similar, and the exchange splitting with SCAN

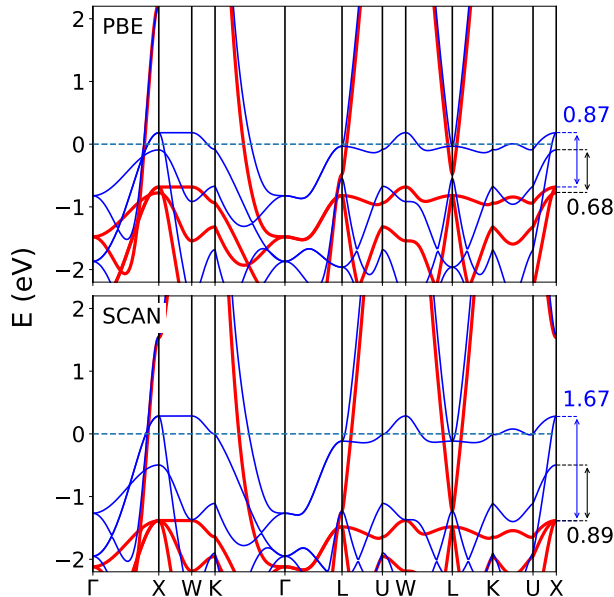


FIG. 6. Band structure of fcc Ni around the Fermi level comparing PBE and SCAN, as obtained from self-consistent calculations with VASP. The Fermi level is at 0 eV and majority (minority) spin are shown as heavy red (light blue). The arrows and numerical values (in eV) give selected exchange splittings at the  $X$  point in eV. Note the similar exchange splittings for PBE and very different exchange splittings for SCAN.

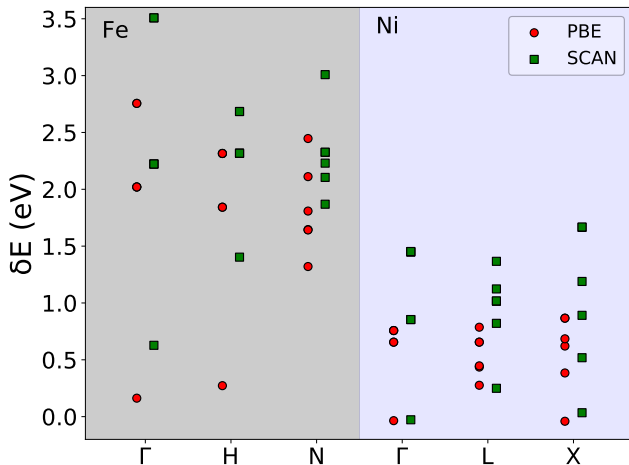


FIG. 7. Exchange splittings of the lowest six bands of bcc Fe and fcc Ni from the band structures of Figs. 5 and 6 at symmetry points.

is larger corresponding to larger magnetizations.

In addition to the overall exchange splitting, there are important differences between the PBE and SCAN band structures, particularly for Ni. The valence electronic structures of Fe and Ni can be roughly described as consisting of bands originating in the  $4s$  orbital and the five  $3d$  states. The lowest band at  $\Gamma$  originates from the  $s$

orbital and disperses rapidly upwards mixing with the  $d$  bands (note that an  $s$  band takes  $p$ -like at the zone boundary, where it is above the Fermi level in these elements). Thus the lowest six bands consist approximately of the  $s$  band and the  $d$  band, which mix away from the  $\Gamma$  point. Fig. 7 shows the exchange splittings of these bands for Fe and Ni at symmetry points. It has been previously noted that SCAN yields enhanced exchange splittings relative to PBE, which then leads to enhanced moments.<sup>19,21</sup> Here we find that this can be strongly orbital dependent, making the connection with the tendency of SCAN to favor integer occupation. This is important because a simple increase in exchange splitting is not enough to give reasonable results for strongly correlated oxides. This is because it will not in itself enhance band gaps if the highest occupied and lowest unoccupied bands are from the same spin. Therefore, orbital occupation dependence beyond a uniform enhancement of exchange splittings is an essential part of noted improvements in the treatment of strongly correlated systems.

In Fe, with the LDA and PBE functionals, the main  $d$  band character is from  $\sim -5$  eV to  $+2$  eV relative to the Fermi energy  $E_F$ , the  $d$  band occupancy is roughly seven electrons, there is partial filling of all the  $d$  orbitals, and the band structure agrees well with experiment aside from some renormalization of the low energy bands, as is well known.<sup>50–54</sup> It should be noted that an enhanced exchange splitting increases the energy separation of occupied and unoccupied  $d$  states, on average, which is a way for favoring integer orbital occupations.

In this regard, Mejia-Rodriguez and Trickey recently presented an analysis of the SCAN functional in comparison with a so-called de-orbitalized version. They find that an orbital related parameter derived from kinetic energy densities implies that SCAN favors spin-polarized states through enhanced exchange splittings.<sup>55</sup> We find that the situation is somewhat more complex because the exchange splitting is enhanced differently for different bands.

The electronic structure of ferromagnetic Ni has been extensively studied. It is roughly described as  $d$  bands and a partially filled  $s$  band, with a  $d$  band occupancy of roughly nine electrons. Differences between LDA and PBE calculations and experiment are well established in Ni. This includes a satellite feature observed in photoemission at  $\sim 6$  eV binding energy relative to the Fermi level,<sup>56</sup> which in any case is a many body effect that cannot be reproduced by Kohn-Sham eigenvalues. Additionally, Ni shows a considerably stronger renormalization of the  $d$  bands, as compared with Fe.<sup>54,57–59</sup> The  $d$  band narrowing in Ni relative to LDA or PBE calculations is accompanied by a decrease in the exchange splitting. These two effects partially cancel as regards the spin magnetization, so that while the exchange splitting is overestimated by a factor of  $\sim 2$  in PBE calculations relative to experiment, the overestimate of the spin magnetization is only  $\sim 10\%$  ( $0.63 \mu_B$  in PBE vs.  $0.57 \mu_B$  in experiment).

The electronic structure near the  $X$  point, where an exchange split  $d$  band occurs near  $E_F$ , has been extensively studied.<sup>54,57,58,60</sup> As seen in Fig. 6, the SCAN and PBE band structures are remarkably different in this region. In particular, the PBE band structure shows similar exchange splittings for the top  $d$  bands. The SCAN band structure on the other hand shows very different exchange splittings for the top bands. The partially filled top  $d$  band has an exchange splitting of 1.67 eV at  $X$ , while the next lower band is exchange split by 0.89 eV. As seen in Fig. 7, the SCAN functional produces a much larger range of exchange splittings in Ni than does the PBE functional. The largest exchange splittings are in the topmost partially filled  $d$  band. Thus SCAN much more strongly differentiates the orbitals in Ni than PBE, again to the effect of favoring integer occupancy through high exchange splittings of partially filled bands. The exchange splittings for fully occupied  $d$ -bands are substantially smaller, which is a behavior different from PBE, for example, where the different  $d$ -bands have much more similar exchange splittings. This feature of SCAN, which as noted above is important for the description of strongly correlated materials, degrades agreement with experiment for Ni.

#### IV. SUMMARY AND CONCLUSIONS

Calculations of the magnetic properties of Fe, Co and Ni with various density functionals show that the SCAN functional is intermediate in accuracy between the standard PBE functional, which provides a generally good description of these materials, and approaches, such as PBE+ $U$  and hybrid functionals that provide a poor description of these ferromagnetic elements, but can describe more localized systems such as Mott insulators. SCAN is more different from the standard PBE than the earlier TPSS and revTPSS meta-GGA functionals, and gives results in worse agreement with experiment for the

magnetism of Fe, Co and Ni.

The SCAN functional differentiates occupied from unoccupied states more strongly than PBE, which is manifested in larger exchange splittings in Fe and Ni, and also in the case of Ni in a greater difference in the exchange splittings between different bands. This can be understood as a greater tendency towards integer orbital occupation, which is an important ingredient in describing atomic systems and small molecules, and also is a key aspect of strongly correlated materials such as Mott insulators.

Thus the challenge of developing a density functional approach that can reliably and predictively treat transition metals and their compounds, including both itinerant and localized systems remains to be solved. This is an important problem not only from the point of view of physics, but also in the context of materials science. This is because in materials science the energies and resulting stabilities of different compounds and phases is important. However, at present, as shown by the present results functionals that describe all the different phases that may be important remain to be developed. For example, none of the practical functionals tested can give a good description of both metallic bcc and fcc Fe, and at the same time Mott insulating oxides. It may be extremely challenging to solve this problem because it is unclear what semilocal information can be used to identify environments that lead to strong itinerancy from those that favor localization.

#### ACKNOWLEDGMENTS

We are grateful for helpful discussions with Jianwei Sun, Fabian Tran and Samuel Trickey. This work was supported by the U.S. Department of Energy, Office of Science, Basic Energy Sciences, Award Number DE-SC0019114.

---

\* singhdj@missouri.edu

<sup>1</sup> J. P. Perdew, A. Ruzsinszky, and J. Tao, J. Chem. Phys. **123**, 062201 (2005).

<sup>2</sup> S. Kummel and L. Kronik, Rev. Mod. Phys. **80**, 3 (2008).

<sup>3</sup> F. Tran, J. Stelzl, and P. Blaha, J. Chem. Phys. **144**, 204120 (2016).

<sup>4</sup> W. E. Pickett, Rev. Mod. Phys. **61**, 433 (1989).

<sup>5</sup> D. J. Singh and W. E. Pickett, Phys. Rev. B **44**, 7715 (1991).

<sup>6</sup> A. Svane, Phys. Rev. Lett. **68**, 1900 (1992).

<sup>7</sup> V. I. Anisimov, J. Zaanen, and O. K. Andersen, Phys. Rev. B **44**, 943 (1991).

<sup>8</sup> V. I. Anisimov, F. Aryasetiawan, and A. I. Lichtenstein, J. Phys.: Condens. Matter **9**, 767 (1997).

<sup>9</sup> A. J. Cohen, P. Mori-Sanchez, and W. Yang, Science **321**, 792 (2008).

<sup>10</sup> P. Mori-Sanchez, A. J. Cohen, and W. Yang, Phys. Rev. Lett. **102**, 066403 (2009).

<sup>11</sup> P. Rivero, I. de P.R. Moreira, and F. Illas, Phys. Rev. B **81**, 205123 (2010).

<sup>12</sup> R. L. Martin and F. Illas, Phys. Rev. Lett. **79**, 1539 (1997).

<sup>13</sup> X. Feng and N. M. Harrison, Phys. Rev. B **70**, 092402 (2004).

<sup>14</sup> J. K. Perry, J. Tahir-Kheli, and W. A. Goddard III, Phys. Rev. B **63**, 144510 (2001).

<sup>15</sup> J. Sun, A. Ruzsinszky, and J. P. Perdew, Phys. Rev. Lett. **115**, 036402 (2015).

<sup>16</sup> Y. Zhang, D. A. Kitchaev, J. Yang, T. Chen, S. T. Dacek, R. A. Samiento-Perez, M. A. L. Marques, H. Peng, G. Ceder, J. P. Perdew, and J. Sun, npj Comput. Mater. **4**, 9 (2018).

- <sup>17</sup> J. Sun, R. C. Remsing, Y. Zhang, Z. Sun, A. Ruzzinszky, H. Peng, Z. Yang, A. Paul, U. Waghmare, X. Wu, M. L. Klein, and J. P. Perdew, *Nature Chemistry* **8**, 831 (2016).
- <sup>18</sup> F. Tran, J. Stelzl, and P. Blaha, *J. Chem. Phys.* **144**, 204120 (2016).
- <sup>19</sup> E. B. Isaacs and C. Wolverton, *Phys. Rev. Mater.* **2**, 063801 (2018).
- <sup>20</sup> C. Lane, J. W. Furness, I. G. Buda, Y. Zhang, R. S. Markiewicz, B. Barbiellini, J. Sun, and A. Bansil, *Phys. Rev. B* **98**, 125140 (2018).
- <sup>21</sup> M. Ekholm, D. Gambino, H. J. M. Jonsson, F. Tasnadi, B. Alling, and I. A. Abrikosov, *Phys. Rev. B* **98**, 094413 (2018).
- <sup>22</sup> S. Jana, A. Patra, and P. Samal, *J. Chem. Phys.* **149**, 044120 (2018).
- <sup>23</sup> Y. Fu and D. J. Singh, *Phys. Rev. Lett.* **121**, 207201 (2018).
- <sup>24</sup> D. H. Lu, M. Yi, S. K. Mo, A. S. Erickson, J. Analytis, J. H. Chu, D. J. Singh, Z. Hussain, T. H. Geballe, I. R. Fisher, and Z. X. Shen, *Nature* **455**, 81 (2008).
- <sup>25</sup> J. P. Perdew, K. Burke, and M. Ernzerhof, *Phys. Rev. Lett.* **77**, 3865 (1996).
- <sup>26</sup> J. Tao, J. P. Perdew, V. N. Staroverov, and G. E. Scuseria, *Phys. Rev. Lett.* **91**, 146401 (2003).
- <sup>27</sup> J. P. Perdew, A. Ruzzinszky, G. I. Csonka, L. A. Constantin, and J. Sun, *Phys. Rev. Lett.* **103**, 026403 (2009).
- <sup>28</sup> J. P. Perdew, A. Ruzzinszky, G. I. Csonka, L. A. Constantin, and J. Sun, *Phys. Rev. Lett.* **106**, 179902 (2011).
- <sup>29</sup> J. Heyd, G. E. Scuseria, and M. Ernzerhof, *J. Chem. Phys.* **118**, 8207 (2003).
- <sup>30</sup> J. Heyd, G. E. Scuseria, and M. Ernzerhof, *J. Chem. Phys.* **124**, 219906 (2006).
- <sup>31</sup> A. V. Krukau, O. A. Vydrov, A. F. Izmaylov, and G. E. Scuseria, *J. Chem. Phys.* **125**, 224106 (2006).
- <sup>32</sup> J. P. Perdew, M. Ernzerhof, and K. Burke, *J. Chem. Phys.* **105**, 9982 (1996).
- <sup>33</sup> C. Adamo and V. Barone, *J. Phys. Chem.* **110**, 6158 (1999).
- <sup>34</sup> G. Kresse and D. Joubert, *Phys. Rev. B* **59**, 1758 (1999).
- <sup>35</sup> G. Kresse and J. Furthmüller, *Phys. Rev. B* **54**, 11169 (1996).
- <sup>36</sup> D. J. Singh and L. Nordstrom, *Planewaves, Pseudopotentials, and the LAPW method, 2nd Ed.* (Springer, Berlin, 2006).
- <sup>37</sup> P. Blaha, K. Schwarz, G. K. H. Madsen, D. Kvasnicka, and J. Luitz, WIEN2k, An augmented plane wave+ local orbitals program for calculating crystal properties (2001).
- <sup>38</sup> K. Schwarz and P. Mohn, *J. Phys. F* **14**, L129 (1984).
- <sup>39</sup> V. L. Moruzzi, P. M. Marcus, K. Schwarz, and P. Mohn, *Phys. Rev. B* **34**, 1784 (1986).
- <sup>40</sup> K. Dewhurst, [Http://elk.sourceforge.net/](http://elk.sourceforge.net/).
- <sup>41</sup> S. L. Dudarev, G. A. Botton, S. Y. Savrasov, C. J. Humphreys, and A. P. Sutton, *Phys. Rev. B* **57**, 1505 (1998).
- <sup>42</sup> B. Himmetoglu, A. Floris, S. de Gironcoli, and M. Cococcioni, *Int. J. Quantum Chem.* **114**, 14 (2013).
- <sup>43</sup> M. Cococcioni and S. de Gironcoli, *Phys. Rev. B* **71**, 035105 (2005).
- <sup>44</sup> F. Tran, P. Blaha, K. Schwarz, and P. Novak, *Phys. Rev. B* **74**, 155108 (2006).
- <sup>45</sup> M. Alfredsson, G. D. Price, C. R. A. Catlow, S. C. Parker, R. Orlando, and J. P. Brodholt, *Phys. Rev. B* **70**, 165111 (2004).
- <sup>46</sup> A. D. Rowan, C. H. Patterson, and L. V. Gasparov, *Phys. Rev. B* **79**, 205103 (2009).
- <sup>47</sup> J. Paier, M. Marsman, K. Hummer, G. Kresse, I. C. Gerber, and J. G. Angyan, *J. Chem. Phys.* **124**, 154709 (2006).
- <sup>48</sup> Y. R. Jang and B. D. Yu, *J. Phys. Soc. Japan* **81**, 114715 (2012).
- <sup>49</sup> P. Janthon, S. Luo, S. M. Kozlov, F. Vines, J. Limtrakul, D. G. Truhlar, and F. Illas, *J. Chem. Theory and Comput.* **10**, 3832 (2014).
- <sup>50</sup> J. Callaway and C. S. Wang, *Phys. Rev. B* **16**, 2095 (1977).
- <sup>51</sup> B. Ackermann, R. Feder, and E. Tamura, *J. Phys. F: Met. Phys.* **14**, L173 (1984).
- <sup>52</sup> A. Santoni and F. J. Himpsel, *Phys. Rev. B* **43**, 1305 (1991).
- <sup>53</sup> J. Schafer, M. Hoinkis, E. Rotenberg, P. Blaha, and R. Claessen, *Phys. Rev. B* **72**, 155115 (2005).
- <sup>54</sup> A. L. Walter, J. D. Riley, and O. Rader, *New J. Phys.* **12**, 013007 (2010).
- <sup>55</sup> D. Mejia-Rodriguez and S. B. Trickey, *cond-mat*, arXiv:1905.01292 (2019).
- <sup>56</sup> L. C. Davis, *J. Appl. Phys.* **59**, R25 (1986).
- <sup>57</sup> D. E. Eastman, F. J. Himpsel, and J. A. Knapp, *Phys. Rev. Lett.* **40**, 1514 (1978).
- <sup>58</sup> F. J. Himpsel, J. A. Knapp, and D. E. Eastman, *Phys. Rev. B* **19**, 2919 (1979).
- <sup>59</sup> A. Liebsch, *Phys. Rev. Lett.* **43**, 1431 (1979).
- <sup>60</sup> D. C. Tsui, *Phys. Rev.* **164**, 669 (1967).